

Probing molecular chirality via electronic transport

F. A. Pinheiro,¹ S. J. S. da Silva,² E. R. Granhen,² and J. Del Nero^{1,2}¹*Instituto de Física, Universidade Federal do Rio de Janeiro, Caixa Postal 68528, Rio de Janeiro 21941-972, RJ, Brazil*²*Departamento de Física, Universidade Federal do Pará, 66075-110 Belém, PA, Brazil*

(Received 7 December 2009; published 29 March 2010)

We investigate electronic molecular transport in several conjugated organic oligomers by means of *ab initio* calculations and nonequilibrium Green's functions method. We demonstrate that the *I-V* characteristics of these molecules constitute a direct manifestation of their degree of molecular chirality, which is calculated using group theory and depends exclusively on the atomic positions. This result shows that electronic current through these specific molecules is strongly correlated with their geometrical degree of chirality.

DOI: [10.1103/PhysRevB.81.115456](https://doi.org/10.1103/PhysRevB.81.115456)

PACS number(s): 73.63.-b, 36.20.Ey, 11.30.Rd, 85.65.+h

Chirality, a term coined by Lord Kelvin to describe the absence of mirror symmetry of some geometrical objects, is an ubiquitous phenomenon in nature.¹ Since the discovery of molecular handedness by Pasteur in 1848 and the birth of stereochemistry, it was realized that molecular chirality has many important implications in several domains of natural sciences.^{1,2} Various optical phenomena have their origin on molecular chirality, such as its classical manifestation, the natural optical activity.^{1,2} The interplay between chirality and magnetism leads to novel optical phenomena, such as the magnetochiral effect.¹⁻⁷ Chirality has also been proposed as an alternative route to generate negative refraction.⁸

Despite its ubiquity and its fundamental and practical importance, the problem of whether chirality can be quantified has only relatively recently been addressed.^{1,9,10} Using group theory, Harris *et al.* defined rotationally invariant pseudo-scalar chiral indexes and applied them to quantify the degree of molecular chirality, showing how they govern a particular observable, such as the pitch of a cholesteric liquid crystal¹⁰ and the optical rotatory power.¹¹ These geometrical chiral indexes were shown to be proportional to the cross sections of magnetochiral light-scattering systems, demonstrating that it is possible to measure the degree of chirality by means of light-scattering experiments.⁵

Symmetry also governs transport properties in a very fundamental way, as stated by the Onsager relations.¹² For instance, in magnetochiral systems symmetry allows an odd dependence in the magnetic field, in contrast to the commonly believed even dependence.^{13,14} The interplay between chirality and electronic molecular transport has been studied in chiral structures, such as carbon nanotubes¹⁵ and DNA strands.¹⁶ Since the pioneering work by Aviram and Ratner,¹⁷ symmetry properties of complex chiral molecules have been explored to generate rectification.¹⁸⁻²⁰ Rectification in chiral "tour wires" molecules has been extensively investigated, including the role of the metallic contacts and intermolecular interactions, by means of first-principles calculations.²¹⁻²³ Molecular chirality and structural properties can induce an asymmetry in electronic transport, also leading to rectification.²⁴ Another important example of the strong correlation between molecular geometry and molecular electronic transport is given in Ref. 25, where the conductance of single biphenyl molecules was experimentally shown to depend on the square of the cosine of the twist angle between the phenyl rings.

Despite the intense research on the effects of molecular geometry and chirality in electronic transport, we are unaware of any study about the connections between quantitative indices of chirality based on molecular geometry and physical observables in electronic transport. This is the aim of this paper, where we demonstrate that this connection exists, by showing that the *I-V* characteristics of well-known molecular devices constitute a direct manifestation of their degree of chirality, calculated using the purely geometrical chiral index proposed in Ref. 10. To accomplish this, we study electronic transport in several organic conjugated oligomers of the family of oligo-(*para*)phenylene-vinylene attached to orthopropyl radical in all phenyl rings (PPV molecules, see for instance Refs. 26 and 27) by means of *ab initio* calculations and nonequilibrium Green's functions (NEGFs) method. PPV polymers are standard chiral organic devices that have been largely used as organic light emission diodes (OLEDs) and organic field emission transistors (OFETs).

Hartree-Fock (HF) derivative calculations with several basis sets have been applied to obtain the charge distribution through the molecule under an external electric field. A full optimization in a closed-shell model for the Roothaan-Hall matrix were utilized, $FC = SCE$, where E is the orbital energy diagonal matrix and S and C are matrices corresponding to the overlap integral and to the coefficient in the linear combination of atomic orbitals, respectively. The Fock matrix F is given by²⁸

$$F_{\mu\nu} = \int d\nu \varphi_{\mu} \left[-\frac{1}{2} \nabla^2 - \sum_{A=1}^M \frac{Z_A}{r_{iA}} \right] \varphi_{\nu} + \sum_{\lambda=1}^K \sum_{\sigma=1}^K P_{\lambda\sigma} \left[(\mu\nu|\lambda\sigma) - \frac{1}{2} (\mu\lambda|\nu\sigma) \right] + V_{\mu\nu}, \quad (1)$$

where the terms correspond to core energy, Coulomb, exchange interactions, and the external fields, respectively. $(\mu\nu|\lambda\sigma)$ and $(\mu\lambda|\nu\sigma)$ are two electronic integrals that may involve up to four different basis functions. The current is given by the instantaneous charge distribution in the molecule for each value of the external electric field. To calculate the charge distribution we have taken into account all molecular orbitals for a realistic description so that every point in the *I-V* curve is an independent optimization of the HF

calculation, as in previous works.^{31,32} The dipole moment p is calculated as a continuous distribution in the r function and averaged over the wave functions of the quantum-mechanical dipole operator, $p = \sum_i r_i + \sum_A Z_A R_A$, where Z_A and R_A are the charge of the nuclear core and the distance between the origin and nucleus A , respectively.

In order to investigate the effects of geometry and chirality on the electronic transport of single molecules, it is desirable to electronically decouple the molecule from the contacts. A strong molecule-contacts coupling significantly modifies the molecular geometry and hence perturbs the electronic structure of the molecules.^{33,34} Experimentally, this decoupling can be achieved by inserting an ultrathin NaCl film between single molecules and a metallic substrate²⁹ or by adsorbing the molecules at low temperatures on hydrogenated Si surfaces.³⁰ As a result, it is possible to probe the individual orbitals of a free molecule by means of scanning-tunneling microscopy imaging. To model this desired decoupling in our transport calculations, we do not explicitly consider the contacts in the *ab initio* calculations.

The description of electronic transport within the NEGF method is based on an effective model composed of left (L) and right (R) electronic reservoirs coupled to the molecular system described as localized levels. Using this model and the equations-of-motion method,³⁵ the NEGF formalism allows one to calculate the current³⁶

$$I_{LR} = \frac{2e}{h} \int T(E) [f_{L/R}(E) - f_{R/L}(E)] dE, \quad (2)$$

where $f_{L/R}(E)$ are the Fermi functions in the leads, $f_{L/R}(E) = \{1 + \exp[(E - \mu_{L/R})/kT]\}^{-1}$, with $\mu_{L/R}$ the chemical potentials, k the Boltzmann constant and T the reservoirs temperature. The transmission coefficient $T(E)$ is given by³⁵

$$T(E) = \sum_i \frac{\Gamma_i^L \Gamma_i^R}{\Gamma_i^L + \Gamma_i^R} \frac{\Gamma_i^L + \Gamma_i^R}{(E - E_i)^2 + \left(\frac{\Gamma_i^L + \Gamma_i^R}{2}\right)^2}, \quad (3)$$

where $\Gamma_i^{L/R}$, treated as parameters in our calculations, are the L and R tunneling rates between the i th molecular level and the contacts. The levels E_i vary with the bias voltage V_e according to $E_i = E_i^0 - \alpha q V_e$, with q the electron charge, and α a parameter that accounts for the asymmetric drop in V_e . The chemical potentials are related to V_e as $\mu_L = \mu_L^0$ and $\mu_R = \mu_R^0 - q V_e$, where the superscript 0 refers to the $V_e = 0$ case. Since we are not interested here in the physics related to Coulomb blockade and electronic correlations, we can employ Eq. (2), which only applies to mean-field calculations, to compute the current. For the same reason, we will restrict the *ab initio* treatment to the HF approximation.

To investigate the interplay between the degree of molecular chirality and electronic transport, we employ the chiral index ψ , introduced to determine the degree of chirality of molecules composed of a single atomic species, defined in Ref. 10 according to

$$\psi = Q^{il} B^{jm} \epsilon_{ijk} S^{klm}, \quad (4)$$

with ϵ_{ijk} the Levi-Civita tensor. In Eq. (4) the tensors S , B , and Q are given by

$$S^{klm} = \sum_{\alpha} \left[r_{\alpha}^k r_{\alpha}^l r_{\alpha}^m - \frac{1}{5} (r_{\alpha}^k)^2 (r_{\alpha}^l \delta^m + r_{\alpha}^l \delta^m + r_{\alpha}^m \delta^{kl}) \right],$$

$$B^{ij} = \psi_B (e_1^i e_1^j - e_2^i e_2^j) \equiv \psi_B \tilde{B}^{ij},$$

$$Q^{ij} = \psi_Q \left(e_3^i e_3^j - \frac{1}{3} \delta^{ij} \right) \equiv \psi_Q \tilde{Q}^{ij}. \quad (5)$$

In Eq. (5) δ^j is the Kronecker delta, \mathbf{r}_{α} is position vector of the atom α relative to the molecular center of mass, and ψ_B and ψ_Q are the eigenvalues corresponding to the matrices \tilde{B} and \tilde{Q} , respectively. The orthonormal basis of vectors $\{\mathbf{e}_1, \mathbf{e}_2, \mathbf{e}_3\}$ specifies the directions of the principal axis of the molecule. ψ , which only depends on the atomic positions, mathematically provides a measure of how much chiral an arbitrary molecule is. As a chiral measure, ψ is a pseudo-scalar invariant under rotations, which guarantees that no rotation of the molecule exists that maps the mirror image of such molecule onto itself. Also, ψ must vanish for achiral configurations, such as bidimensional structures and molecules composed of less than four atoms.¹⁰ The definition of chiral indexes for molecules composed of different atomic species exists and takes into account different weight functions that reflect the atomic weight.¹⁰ However, for the conjugate organic oligomers, the difference between the values of these indexes and ψ [Eq. (4)] is negligible due to the small atomic weight of the hydrogen relative to the carbon atoms.

The electronic transport properties of the chiral PPV molecules are discussed in Fig. 2, where the current, calculated by both HF *ab initio* and NEGF methods, is calculated as a function of external voltage V_e applied in the direction of the molecular backbone for two chiral PPV molecules, namely, the PPV-|| and PPV-anti|| (Fig. 1). The PPV-anti|| corresponds to a different stable configuration of the PPV-||, where two propyl radicals are attached to the opposite side of the molecular backbone. Figure 2 demonstrates that the agreement between the two independent methods is excellent, as it has been reported in several others molecular devices,^{31,32} confirming the validity and accuracy of our transport calculations. The NEGF model, where two molecular levels $E_{i=1,2}$ are taken into account, already captures the full electronic dynamics present in the *ab initio* calculations. In the bottom panel of Fig. 2 the molecular levels $E_{i=1,2}$ and the chemical potentials at the right and left ends of the molecule, $\mu_{R,L}$, are shown as a function of V_e . We take into account levels of different widths by asymmetric tunneling barriers. Electronic transport is facilitated whenever the resonant conditions $E_i = \mu_L$ and $E_i = \mu_R$ are reached (indicated by vertical arrows in the bottom panels of Fig. 2), depending on whether the applied bias is forward or reverse. This result confirms that the molecular electronic states are accessed during the transport process so that the current is determined by the electronic flow through the molecular backbone. Hence transport is given by hopping of electrons from the first contact to the molecular electronic states and then to second contact.

The connection between electronic transport and the degree of molecular chirality is studied in Fig. 3, where the modulus of the current $|I|$, calculated by the HF *ab initio*

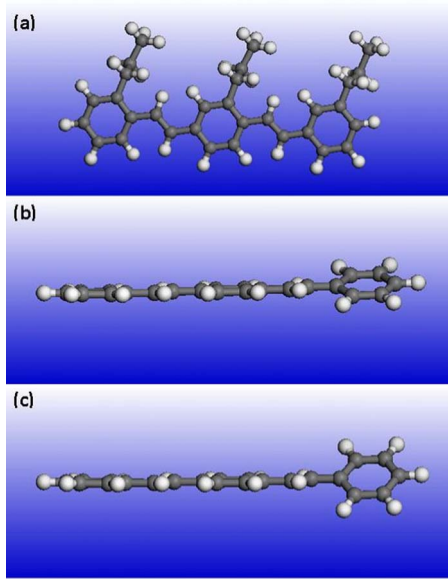


FIG. 1. (Color online) Schematic view of the PPV oligomers. Parallel conformation (PPV-||) with (a) front view and lateral view with dihedral angle of (b) 15 and (c) 30° [the C_3H_7 radicals were removed from (b) and (c) for better view] under external electric field.

method, and the chiral index ψ , calculated using Eqs. (4) and (5), are exhibited as a function of V_e for the PPV-|| and PPV-anti|| molecules (Fig. 1). Figure 3 demonstrates that ψ is strongly correlated with $|I|$, for both molecules exhibited. We have extensive numerical evidence that this result is valid for the whole family of organic conjugated oligomers. We conclude that electronic transport represents a direct manifestation of the geometrical degree of molecular chirality in these specific systems. The variation in V_e changes the atomic positions to generate the most stable molecular configuration. Hence there is a set of atomic positions and a different value of ψ for each value of V_e . As V_e varies, we have identified three major stable molecular structural configurations that manifest themselves as three characteristic behaviors of both ψ and $|I|$. For the PPV-|| molecule they are: (i) for $-2.4 < V_e < 2.2$ V the molecule is quasiplanar (dihedral angle θ of few degrees) (see Fig. 1) and has an aromatic character; (ii) for $-3.6 < V_e < -2.4$ V and for $V_e > 2.2$ V the molecule is also quasiplanar and resonates, stabilizing into a quinoidal configuration; (iii) for $V_e < -3.6$ V a new resonance occurs, giving rise to a change in the dihedral angle of $\theta \sim 40^\circ$. These three behaviors are also found for the PPV-anti|| molecule, but for slightly different values of V_e . Configuration (iii) is characterized by a more pronounced increase of $|I|$ and ψ and by the fact that the molecules acquire a large out-of-plane component. Thus ψ , and consequently $|I|$, increase abruptly since the chiral index of a 3D molecule is expected to be much larger than that of a quasiplanar one.

In Fig. 4 the modulus of the molecular electric-dipole moment p and ψ are calculated as a function of V_e , for both PPV-|| and PPV-anti|| molecules. p and ψ are also strongly correlated, which can be explained by the fact that, when a molecule has a nonvanishing electric-dipole moment, it is possible to relate ψ to p .¹⁰ p exhibits the three characteristic

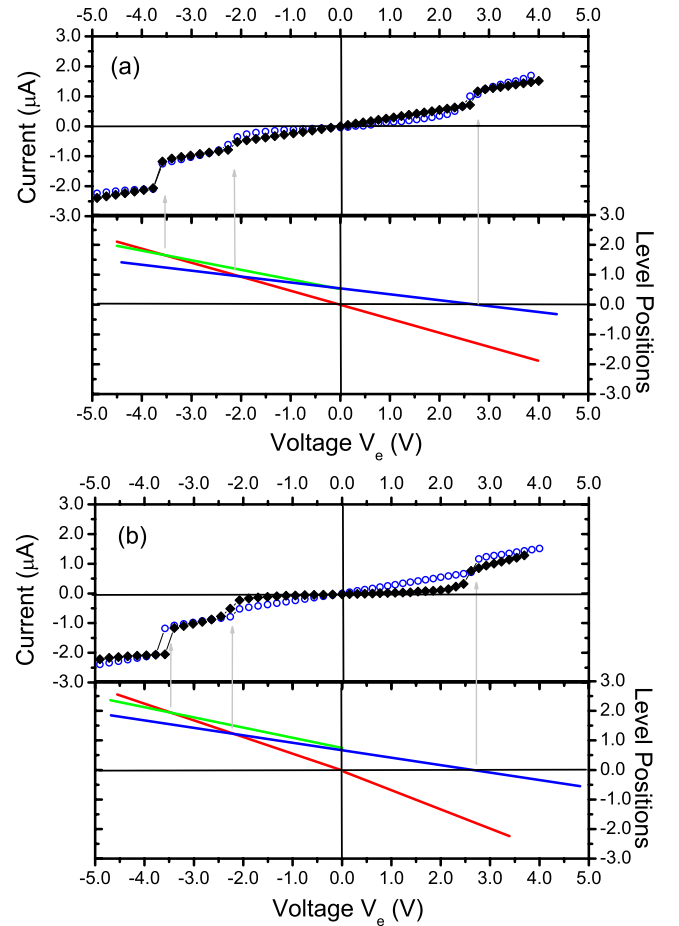


FIG. 2. (Color online) Transport properties of the PPV molecules. (a) The current (I) as a function of the external voltage V_e for the PPV molecule in the parallel (||) configuration, calculated by both *ab initio* HF (open blue circles) and NEGF (full black diamonds) methods; In the bottom panel, we show the localized levels, E_1 (solid blue line), E_2 (solid green line), and the chemical potentials $\mu_L=0$ (black horizontal line), and $\mu_R=-eV_e$ (red line) against V_e . The resonant conditions are indicated by vertical arrows. The parameters for the NEGF calculations are $\Gamma^L=0.95$ eV, $\Gamma^R=0.68$ eV, and room temperature. (b) The same of Fig. 2(a) but for the PPV molecule in the antiparallel (anti||) configuration.

behaviors (i)–(iii) reported for the current in Fig. 3. Recalling that ψ and I are strongly related from Fig. 3, this result shows that p and I are also correlated.

The analysis of the effects of the molecular dipole on the I - V characteristics, which have been studied in Refs. 18 and 37, helps to understand in physical terms the connection between ψ and I . Indeed, the presence of an interface molecular dipole in heterojunctions was experimentally shown to affect the charge distribution in between the junction and hence modify the potential difference.¹⁸ To model this effect, one can describe electronic molecular transport as a tunneling process in which the effective height of junctions's barrier, Φ_{eff} , is altered by the molecular dipole contribution, Φ_{dip} ,¹⁸

$$q\Phi_{\text{eff}} = q\Phi_{\text{junct}} - q\Phi_{\text{dip}}, \quad (6)$$

where Φ_{junct} is the contribution of the contacts to the barrier height (for example, in the case of metallic contacts Φ_{junct}

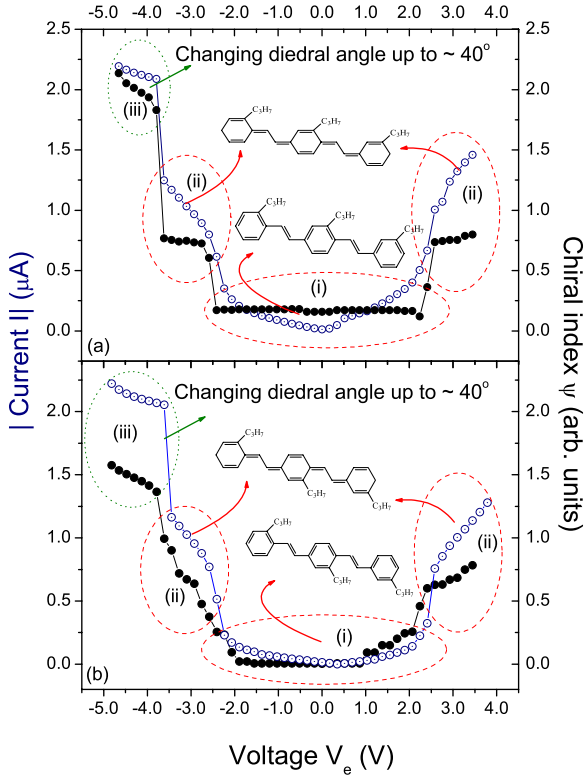


FIG. 3. (Color online) Modulus of current $|I|$ (left vertical axis), calculated by the *ab initio* (open blue circles), and chiral index ψ (right vertical axis, full black circles) as a function of external voltage V_e for PPV molecules in (a) parallel (\parallel) and (b) antiparallel ($\text{anti}\parallel$) configurations. The molecules exhibit three structural configurations: (i) quasiplanar and aromatic, (ii) quasiplanar and quinoidal, and (iii) three-dimensional (3D) and quinoidal.

corresponds to the metal work function). Φ_{dip} is given by $\Phi_{\text{dip}} = (P \cos \theta) / \epsilon \epsilon_0$, where P is the total dipole moment per unit of area, ϵ is the effective molecular dielectric permittivity, ϵ_0 is the vacuum dielectric permittivity, and θ is the angle between the \mathbf{P} and the normal to the contacts; i.e., θ is the average dihedral angle. The current through the barrier is¹⁸

$$I = I_0 \exp\left(\frac{-q\Phi_{\text{eff}}}{kT}\right), \quad (7)$$

where I_0 is related to the ordinary thermionic emission formula.³⁸ Equation (7) was shown to satisfactorily describe the experimental I - V characteristics in heterojunctions with adsorbed molecules at the interface.¹⁸ Since our transport calculations were performed at room temperature, so that $q\Phi_{\text{dip}} \ll kT$, Eqs. (6) and (7) yield

$$I \simeq I_0 \exp\left(\frac{-q\Phi_{\text{junct}}}{kT}\right) \left(1 + \frac{qP \cos \theta}{kT \epsilon \epsilon_0}\right). \quad (8)$$

Equation (8) shows that, in a first approximation, I is proportional to the molecular dipole moment, which explains the linear dependence of I on p found in our transport calculations. Since ψ is proportional to p from Fig. 4 and Ref. 10, the above argument also explains why ψ is correlated with

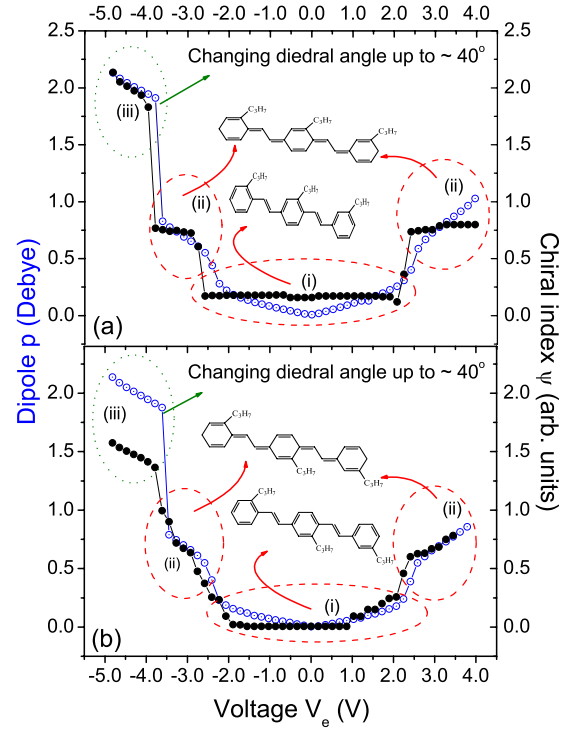


FIG. 4. (Color online) Dipole moment p (left, open blue circles) and chiral index ψ (right, full black circles) as a function of external voltage V_e for PPV molecules in (a) parallel (\parallel) and (b) antiparallel ($\text{anti}\parallel$) configurations, exhibiting the same three characteristic behaviors presented in Fig. 3.

both I and p , as demonstrated in Figs. 3 and 4. In view of Eq. (8), it is clear the dependence of I on the dihedral angle θ (Fig. 3), which can be interpreted as a torsional parameter that governs the behavior of ψ in PPV molecules. Finally, our findings suggest that electronic transport and natural optical activity in molecular systems are sensitive to chirality because they both depend on the molecular dipole moment, which is in turn related to the degree of chirality.¹⁰ Indeed, the natural optical activity of molecules, both in refraction and absorption, is proportional to the electric-dipole moment.¹

In conclusion, we have investigated the connection between electronic transport in conjugated organic oligomers (PPV molecules) and their geometrical degree of chirality. We have demonstrated that the I - V characteristics and the dipole moment of these structures are a direct manifestation of their degree of chirality. We suspect that the connection between electronic transport and the degree of chirality is valid not only for PPV molecules but also to other molecules, provided the electronic transport is affected by the molecular electric dipole. This aspect is under investigation and will be reported soon.

We thank F. M. Souza, C. H. Lewenkopf, R. B. Capaz, and B. Koiller for fruitful discussions. This work was partially supported by the Brazilian agencies CNPq, FAPERJ, FAPESPA, Rede Nanotubos de Carbono/CNPq, PPGF, PPGE, and INCT Nanomateriais de Carbono/CNPq.

- ¹G. H. Wagnière, *On Chirality and the Universal Asymmetry* (Wiley-VCH, Zürich, 2007).
- ²L. Barron, *Molecular Light Scattering and Optical Activity* (Cambridge University Press, Cambridge, 2004).
- ³G. L. J. A. Rikken and E. Raupach, *Nature* (London) **390**, 493 (1997).
- ⁴G. L. J. A. Rikken and E. Raupach, *Nature* (London) **405**, 932 (2000).
- ⁵F. A. Pinheiro and B. A. van Tiggelen, *Phys. Rev. E* **66**, 016607 (2002).
- ⁶F. A. Pinheiro and B. A. van Tiggelen, *J. Opt. Soc. Am. A Opt. Image Sci. Vis* **20**, 99 (2003).
- ⁷C. Train, R. Gheorghe, V. Krstic, L. M. Chamoreau, N. S. Ovanesyan, G. L. J. A. Rikken, M. Gruselle, and M. Verdaguer, *Nature Mater.* **7**, 729 (2008).
- ⁸J. B. Pendry, *Science* **306**, 1353 (2004).
- ⁹M. A. Osipov, B. T. Pickup, and D. A. Dunmur, *Mol. Phys.* **84**, 1193 (1995).
- ¹⁰A. B. Harris, R. D. Kamien, and T. C. Lubensky, *Rev. Mod. Phys.* **71**, 1745 (1999).
- ¹¹M. S. Spector, S. K. Prasad, B. T. Weslowski, R. D. Kamien, J. V. Selinger, B. R. Ratna, and R. Shashidhar, *Phys. Rev. E* **61**, 3977 (2000).
- ¹²L. D. Landau and E. M. Lifshitz, *Statistical Physics* (Pergamon, Oxford, 1980).
- ¹³G. L. J. A. Rikken, J. Fölling, and P. Wyder, *Phys. Rev. Lett.* **87**, 236602 (2001).
- ¹⁴V. Krstic, S. Roth, M. Burghard, K. Kern, and G. L. J. A. Rikken, *J. Chem. Phys.* **117**, 11315 (2002).
- ¹⁵Z. Yao, H. W. C. Postma, L. Balents, and C. Dekker, *Nature* (London) **402**, 273 (1999).
- ¹⁶R. G. Endres, D. L. Cox, and R. R. P. Singh, *Rev. Mod. Phys.* **76**, 195 (2004).
- ¹⁷A. Aviram and M. A. Ratner, *Chem. Phys. Lett.* **29**, 277 (1974).
- ¹⁸A. Vilan, A. Shanzer, and D. Cahen, *Nature* (London) **404**, 166 (2000).
- ¹⁹F. Schindler, J. M. Lupton, J. Muller, J. Feldmann, and U. Scherf, *Nature Mater.* **5**, 141 (2006).
- ²⁰I. I. Oleynik, M. A. Kozhushner, V. S. Posvyanskii, and L. Yu, *Phys. Rev. Lett.* **96**, 096803 (2006).
- ²¹K. Stokbro, J. Taylor, and M. Brandbyge, *J. Am. Chem. Soc.* **125**, 3674 (2003).
- ²²J. Taylor, M. Brandbyge, and K. Stokbro, *Phys. Rev. Lett.* **89**, 138301 (2002).
- ²³J. Taylor, M. Brandbyge, and K. Stokbro, *Phys. Rev. B* **68**, 121101(R)(2003).
- ²⁴A. S. Martin, J. R. Sambles, and G. J. Ashwell, *Phys. Rev. Lett.* **70**, 218 (1993).
- ²⁵L. Venkataraman, J. E. Klare, C. Nuckolls, M. S. Hybertsen, and M. L. Steigerwald, *Nature* (London) **442**, 904 (2006).
- ²⁶E. Hendry, J. M. Schins, L. P. Candeias, L. D. A. Siebbeles, and M. Bonn, *Phys. Rev. Lett.* **92**, 196601 (2004).
- ²⁷S. Mazumdar, *Science* **288**, 630 (2000).
- ²⁸M. Dragoman and D. Dragoman, *Nanoelectronics: Principles and Devices* (Artech House, Boston, 2006).
- ²⁹J. Repp, G. Meyer, S. M. Stojkovic, A. Gourdon, and C. Joachim, *Phys. Rev. Lett.* **94**, 026803 (2005).
- ³⁰A. Bellec, F. Ample, D. Riedel, G. Dujardin, and C. Joachim, *Nano Lett.* **9**, 144 (2009).
- ³¹A. Saraiva-Souza, F. M. de Souza, V. F. P. Aleixo, E. C. Girao, J. Mendes, V. Meunier, B. G. Sumpter, A. G. Souza, and J. Del Nero, *J. Chem. Phys.* **129**, 204701 (2008).
- ³²A. Saraiva-Souza, R. M. Gester, M. A. L. Reis, F. M. Souza, and J. Del Nero, *J. Comput. Theor. Nanosci.* **5**, 2243 (2008).
- ³³J. A. Malen, P. Doak, K. Baheti, T. D. Tilley, A. Majumdar, and R. Segalman, *Nano Lett.* **9**, 3406 (2009).
- ³⁴S. Y. Quek, H. J. Choi, S. G. Louie, and J. B. Neaton, *Nano Lett.* **9**, 3949 (2009).
- ³⁵H. Haug and A.-P. Jauho, *Quantum Kinetics in Transport and Optics of Semiconductors*, 2nd ed. (Springer, New York, 2008).
- ³⁶A. Hernández, V. M. Apel, F. A. Pinheiro, and C. H. Lewenkopf, *Physica A* **385**, 148 (2007).
- ³⁷R. C. Hoft, N. Armstrong, M. J. Ford, and M. B. Cortie, *J. Phys.: Condens. Matter* **19**, 215206 (2007).
- ³⁸E. H. Rhoderick and R. H. Williams, *Metal-Semiconductor Contacts*, 2nd ed. (Clarendon Press, Oxford, 1988).